Article:
Moldovan, AA orcid.org/0000-0003-2776-3879, Penchev, RY, Hammond, RB orcid.org/0000-0003-0691-7779 et al. (4 more authors) (2021) Automated In Silico Energy Mapping of Facet-Specific Interparticle Interactions. Crystal Growth and Design, 21 (10). pp. 5780-5791. ISSN 1528-7483

https://doi.org/10.1021/acs.cgd.1c00674

Supporting Information: Automated In-Silico Energy Mapping of Facet Specific Inter-Particle Interactions

Alexandru A. Moldovan [†,‖,]*, *Radoslav Y. Penchev* [‡], *Robert B. Hammond* [§], *Jakub P. Janowiak* [†], *Thomas E. Hardcastle* [†,‖], *Andrew G. P. Maloney* [‖], *and Simon D. A. Connell*[⊥,]*

† Center for Doctoral Training, Complex Particulates Products and Processes, School of Chemical and Process Engineering, University of Leeds, Leeds, UK

‡ Pfizer, Drug Product Design, Sandwich, Kent, UK

§ School of Chemical and Process Engineering, University of Leeds, Leeds, UK

‖ Cambridge Crystallographic Data Centre, Cambridge, UK

⊥ School of Physics and Astronomy, University of Leeds, Leeds, UK

Optimized Structure Lattice Parameters

Table S1: Crystallographic information of Paracetamol crystal structure HXACAN28 pre and post geometry optimization. Z describes the number of asymmetric units in the unit cell and Z' the number of molecules in the asymmetric units.

Cell Parameters	Initial Structure	Final Optimised Structure
a (Å)	7.077(2)	7.4370(1)
b (Å)	9.173(2)	9.348(2)
c (Å)	11.574(4)	11.393(8)
α (°)	90	90
β (°)	97.9	97.9
ϒ (°)	90	90
Z = 4	Z' = 1	

Construction of atoms during optimisation and interaction energy calculations

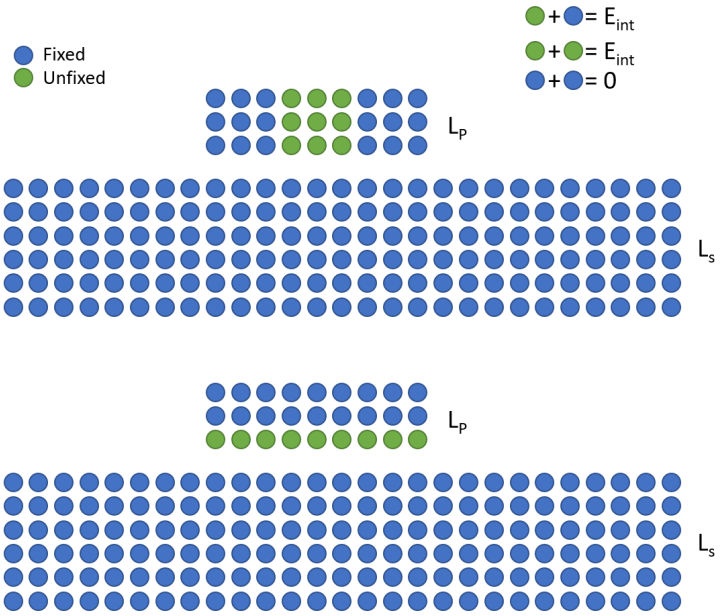

Figure S1 - Illustration of the approaches used in calculating the production E_{int} (top) and E_{int} as part of the optimum separation scan (bottom). The use of the peripheral atoms on the bottom figure allows for the detection of collision even if the lattice types of the surfaces are mismatched.

Algorithm for finding local minimum of two separating surfaces

Figure S2 illustrates the initial steps once the surfaces have been created and the centroids overlapped. As it can be seen in some situations the layers could be interdigitated to such degree that separating them will yield a local minimum immediately after moving the layer (point 2). To speed up and assist the steepest descent style algorithm, the layers are separated by 1.5 A once centroids have been overlapped.

The developed algorithm finds the local minimum between the two surfaces with the least number of steps required. Whilst carrying out a steepest decent method would yield similar results, the optimisation could oscillate around the minimum for too many iterations, and as each calculation is expensive, we saw it fit to reduce the number of iterations required.

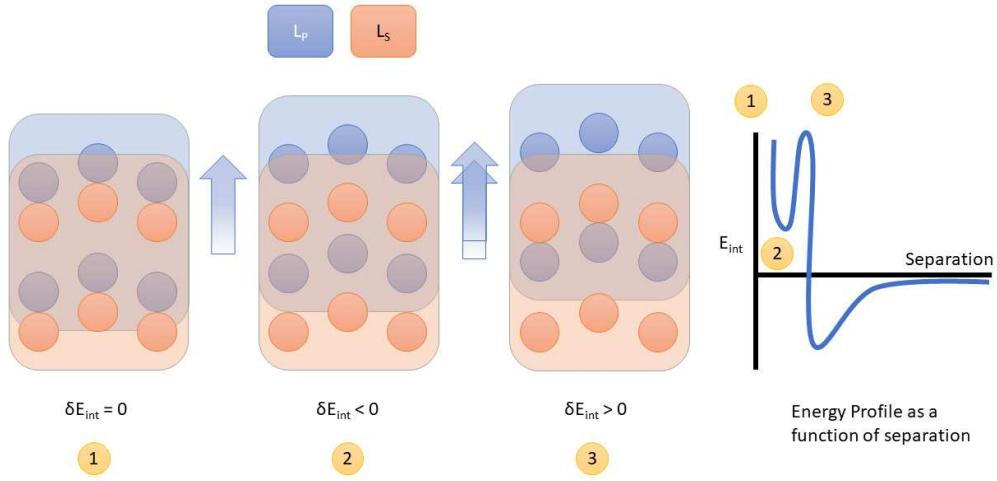

Figure S2 - Diagram illustrating the overlapping that occurs when separating two layers from overlapped centres of geometries. As L_P (blue box) separates (1) from L_S (orange box) the energy (δE_{int}) reduces and a local minimum is created once the layer moves again (2). Due to this, the model initially takes 1.5 A to clear the local minimum and start at point (3).

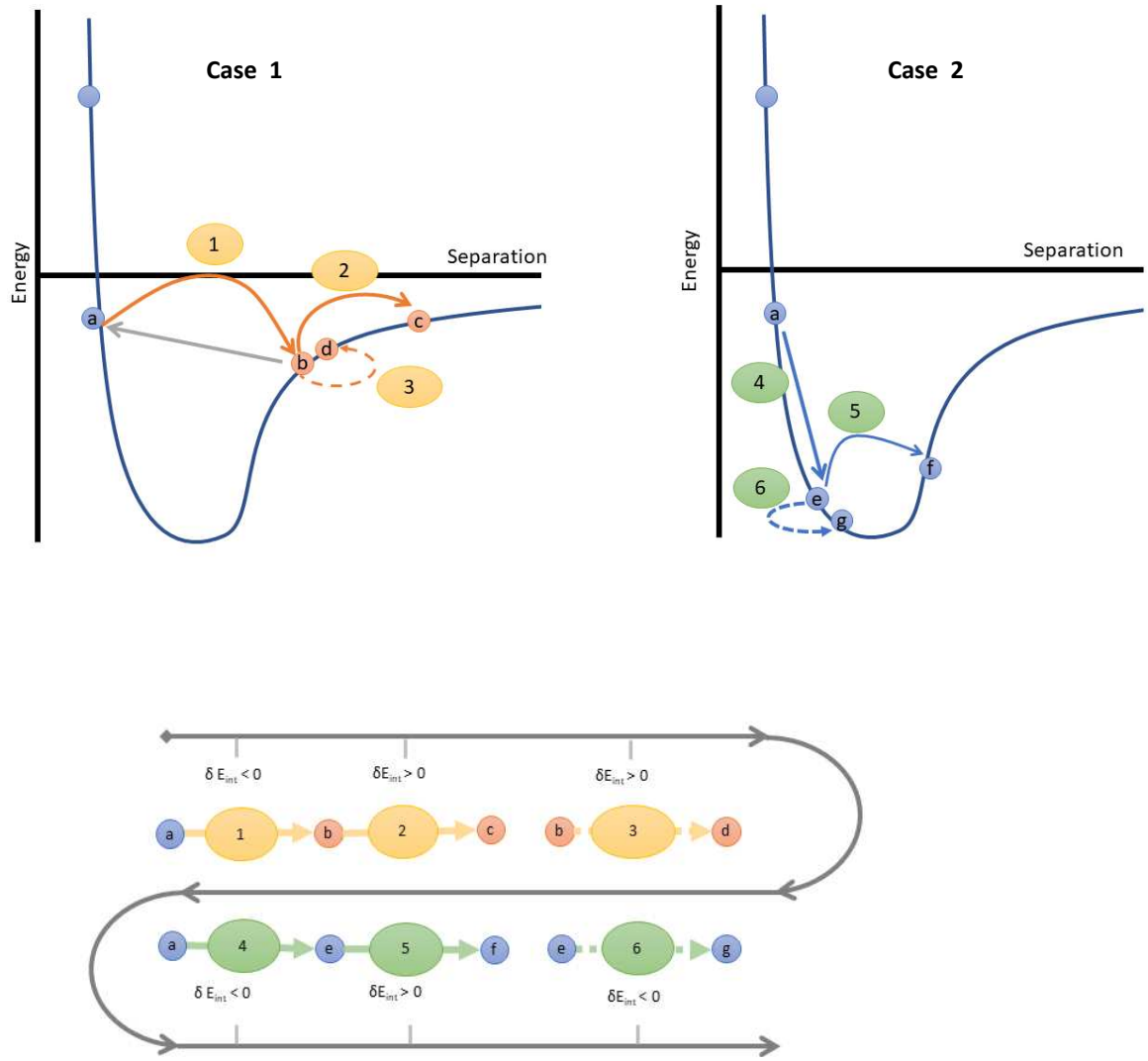

Figure S3 - Separation steepest descent algorithm. Case 1 shows the situation where the step size is largely overshot. Case 2 illustrates the situation where the step size is overshot next to the minima. Bottom diagram illustrates the changes in δE_{int} with each change of position for both cases and process by which the algorithm moves from case 1 to case 2.

This optimisation takes advantage of the LJ type curve by distinguishing where on the curve the current energy position can be found. During optimisation, the energetical trajectory can be summarised by two cases.

Figure S3a shows the possible cases:

Case 1: The minimum is overshot moving from *a* -> *b,* thus $\delta E_{int} < 0$. The following step taken between *b* -> *c* yields a $\delta E_{int} > 0$. If a single repulsive step has been detected the algorithm will go back to position *b* and take a step size of 0.001 A - this is treated as a "scouting step". Essentially determining if the forward point is on a positive or negative gradient.

If $\delta E_{int} > 0$, the algorithm distinguished the current position to be on the right of E_{int} minimum. Whereas, if $\delta E_{int} < 0$ it is to the left and normal step sizes are resumed.

In the given example, because the energy minimum has been passed, the layer moves back to position *a*. From this position, another step is taken with a new step size calculated by halving the size constant (*S*) and thus making a smaller step size than the initial a -> b. Figure S2b shows the flow of conditions required to move to different positions.

Case 2: Moving positions *g* -> *f* where $\delta E_{int} > 0$, overshoots the minimum. As previously mentioned, due to a positive δE_{int} being detected, the algorithm goes back to point *e* and takes a "scouting step" of 0.001Å. Calculating *e* -> *g* as $\delta E_{int} < 0$, after which the algorithm resumes normal descent.

Figure S3b illustrates the flow of steps as the algorithm moves from one step to the next.

Evidence of negligible difference when flipping surfaces A/B -> B/A

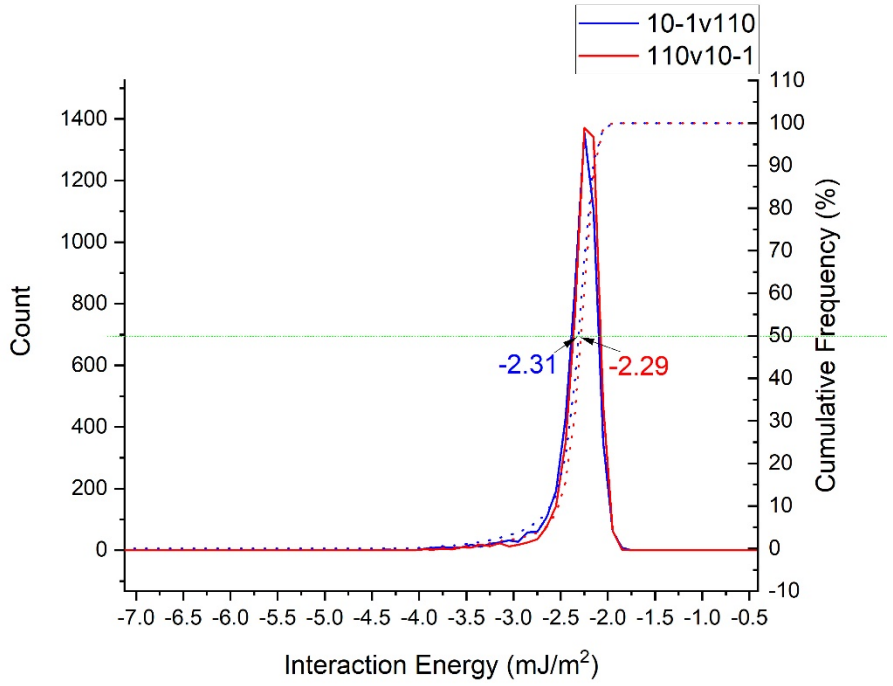

Figure S4 - Distribution of interaction energy of 10-1/110 (blue) and 110/10-1 (red) illustrating that flipping the two surfaces has negligible difference on the interaction energy. Energies were calculated during the convergence step where the top layer was 1 d-spacing thick.

Contributions of individual energy components towards surface-surface interactions

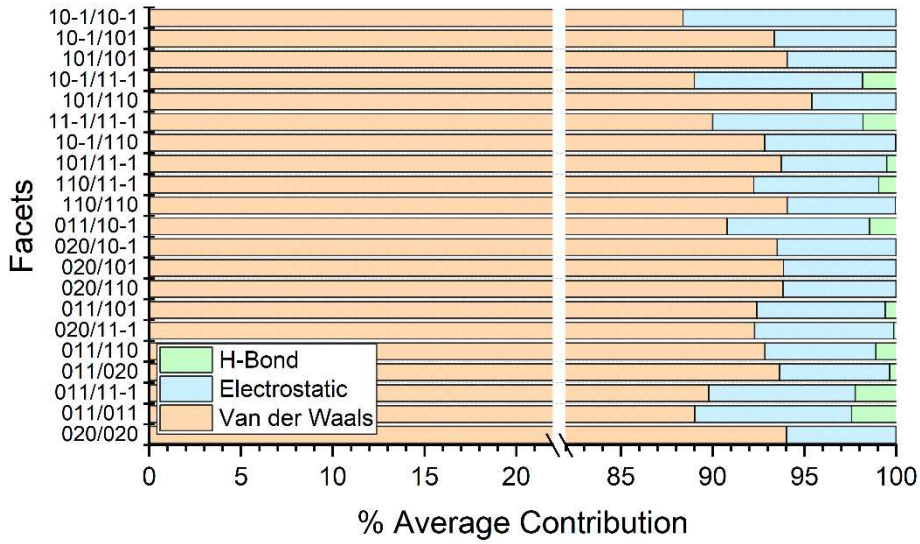

Figure S5 - Average contribution % from each component energy towards the total interaction energy for specific facet-facet interactions of Para-Para.

Averaged Interaction energies for paracetamol/paracetamol interactions

Table S2 - Average interaction energy for each probe and the standard error across all surface-surface interactions. Ranked in order of descending anisotropy factor.

Surface	Average Interaction Energy (mJ/m^2)	Standard Error (mJ/m^2)
{011}	-30.604	3.684
{101}	-45.323	3.840
{10-1}	-45.780	3.909
{020}	-31.309	2.199
{110}	-41.959	3.397
{11-1}	-43.055	3.684

Energy conversion equation

All values were calculated in kcal mol^{-1} and were converted into mJ m^{-2} using Equation S1, where k_a and k_b are the conversion factors for $Å^2$ to m^2 (10^{20}) and kcal to mJ ($4.184x10^6$) respectively.

$$\frac{kcal}{mol\,A^2} \times \frac{k_a k_b}{N_A} = \frac{mJ}{m^2} \qquad \text{Equation S1}$$